New insights into the mechanism of electrotransfer of small nucleic acids

Rūta Palepšienė [a], Aswin Muralidharan [b,c], Martynas Maciulevičius [a], Paulius Ruzgys [a], Sonam Chopra [a], Pouyan E. Boukany [d], Saulius Šatkauskas [a,*]

[a] Research Institute of Natural Sciences and Technology, Vytautas Magnus University, Universiteto str. 10, Akademija, Kaunas district LT-53361, Lithuania
[b] Department of Bionanoscience, Delft University of Technology, Van der Maasweg 9 2629 HZ Delft, Netherlands
[c] Kavli Institute of Nanoscience, Delft University of Technology, Van der Maasweg 9 2629 HZ Delft, Netherlands
[d] Department of Chemical Engineering, Delft University of Technology, Van der Maasweg 9 2629 HZ Delft, Netherlands

ABSTRACT

RNA interference (RNAi) is a powerful and rapidly developing technology that enables precise silencing of genes of interest. However, the clinical development of RNAi is hampered by the limited cellular uptake and stability of the transferred molecules. Electroporation (EP) is an efficient and versatile technique for the transfer of both RNA and DNA. Although the mechanism of electrotransfer of small nucleic acids has been studied previously, too little is known about the potential effects of significantly larger pDNA on this process. Here we present a fundamental study of the mechanism of electrotransfer of oligonucleotides and siRNA that occur independently and simultaneously with pDNA by employing confocal fluorescence microscopy. In contrast to the conditional understanding of the mechanism, we have shown that the electrotransfer of oligonucleotides and siRNA is driven by both electrophoretic forces and diffusion after EP, followed by subsequent entry into the nucleus within 5 min after treatment. The study also revealed that the efficiency of siRNA electrotransfer decreases in response to an increase in pDNA concentration. Overall, the study provides new insights into the mechanism of electrotransfer of small nucleic acids which may have broader implications for the future application of RNAi-based strategies.

1. Introduction

Electroporation (EP) is a biophysical technique designed for *in vitro* and *in vivo* delivery of bioactive compounds. This non-viral method is based on the direct application of an external electric field to target cells or tissues resulting in transient permeabilization of the plasma membrane and entry of molecules into otherwise impermeable cells [1,2]. The method has been demonstrated to be a safe and cost-effective alternative to other delivery methods and has been successfully employed for the electrotransfer of small molecules, such as propidium iodide, chemotherapeutic agents (bleomycin, cisplatin), and various-sized nucleic acids (RNA and DNA) [3–19].

Small interfering RNA (siRNA) molecules are short, typically 20–25 base pair (bp) long, double-stranded RNA molecules. siRNA acts by binding to a protein complex called the RNA-induced silencing complex (RISC), which, in turn, targets complementary messenger RNA (mRNA) molecules by cleaving them and generating mRNA fragments that are

completely destructed by cellular nucleases. This process of sequence-specific silencing is referred as RNA interference (RNAi) [20–22]. Several types of oligonucleotides, such as antisense oligonucleotides (ASOs), can also degrade mRNA and precisely suppress specific genes in both the nucleus and cytoplasm [23].

Both siRNA and oligonucleotides have shown great therapeutic potential in anticancer and gene therapy [24–27]. However, the limited cellular uptake and stability of the molecules hinder the clinical progress of RNAi. Effective delivery is a major obstacle to the progress of RNAi-based therapies [28]. Among different strategies electroporation demonstrated efficacy for enhanced delivery of molecules [7,16,17]. According to the generally accepted mechanism of electrotransfer, negatively charged siRNA molecules exhibit electrophoretic movement upon exposure to an electric field, leading to direct access to the cytoplasm on the cathode-oriented side of the cell. When the exposure to the electric field is canceled, intracellular uptake of siRNAs is terminated, with the molecules localizing exclusively within the cytoplasm and not

entering the nucleus [29]. A mechanism for intra-nuclear entry has been described for short oligonucleotides, but the only difference is that they rapidly localize within the nucleus after EP [30].

In comparison to the therapeutic applications of the electrotransfer of siRNA and oligonucleotides, the transfer of DNA has shown great feasibility for treatment in various biomedical approaches [31,32]. Studies have demonstrated DNA electrotransfer is a complex process, that begins with the interaction between DNA and the cell membrane, forming distant aggregates. Since the electrotransfer of pDNA is controlled by electrophoresis, the formation of these structures is observed exclusively on the side of the cells facing the cathode [33,34]. Within minutes after electroporation (EP), these aggregates cross the membrane and migrate to the nucleus [35–40].

There is growing evidence that the combined transfer of two or more types of molecules using EP can significantly affect the efficiency of transfer. The interaction of DNA with the plasma membrane during EP has been associated with the enhanced delivery of small molecules (<1.5 nM in size and < 4 kDa of molecular mass), including Lucifer yellow [41], and bleomycin [42], as well as facilitated calcein release from cells [43]. Previous studies have also shown that the co-transfer of the large vector CRISPR-GFP with small vectors increased transfection efficiency [44]. It has been hypothesized that the observed processes are caused by a prolonged period of pore resealing, inhibition of electrotransfer-induced plasma membrane damage, or DNA-mediated endocytosis [43,45,46], however, the exact mechanism is still under investigation. Considering the influence of pDNA on the electrotransfer of both small and large molecules, it is conceivable that the cellular uptake of small nucleic acids, such as oligonucleotides or siRNA, could also be significantly affected. In this study, we investigated the electrotransfer of oligonucleotides and siRNA using confocal fluorescence microscopy at a single-cell level. In addition, we analyzed the effects of simultaneous siRNA and pDNA electrotransfer on the cellular uptake of siRNA. Therefore, in this study, we present an updated overview of the current mechanism of oligonucleotide and siRNA electrotransfer. Our study provides empirical evidence that cellular uptake of both molecules is determined by the combination of electrophoresis and post-pulsation diffusion, followed by subsequent entry into the nucleus within 5 min after EP. For the first time in the field of EP, we have shown that the presence of pDNA during EP negatively affects the efficiency of siRNA electrotransfer.

2. Materials and methods

2.1. Cell culture

Chinese Hamster Ovary (CHO-K1) cells (European Collection of Authenticated cell cultures, 85050302) were cultivated in Ham's F-12 K culture medium (Kaighn's Medium F12K, Gibco™, Gaithersburg, MD, USA), supplemented with 10 % Fetal Bovine Serum (FBS) (Gibco™, Gaithersburg, MD, USA), and 1 % penicillin–streptomycin solution (Sigma-Aldrich, St. Louis, MO, USA) in a humidified incubator at 37 °C and 5 % CO_2. Cells were cultured every 2–3 days and 24 h before experiments. After removal of the growth medium, cells were washed with $1\times$ (phosphate-buffered saline) PBS (Sigma-Aldrich, St. Louis, MO, USA). 0.25 % Trypsin-EDTA solution (1x) (Sigma-Aldrich) was then added to the cell monolayer and incubated at 37 °C for 4 min. Cells were then resuspended in 2 ml of medium, centrifuged at 145 g 2 min, and counted using a hemocytometer (Paul Marienfeld GmbH & Co. KG). For microscopy experiments, 0.2×10^5 cells were seeded into a 4-chamber microscope coverslip (Ibidi, Graefelfing, Germany) 24 h before the experiment.

2.2. Molecules

A 35nt long single-stranded DNA oligonucleotide labeled at the 5′ end with Alexa 488 dye (5′GAATTCGGCTGTACTATATGTCTAT GCACTATTTG 3′) (Invitrogen, Washington DC, USA) and a ~ 21 bp long double-stranded siRNA labeled with Alexa 555 dye (BLOCK -iT™ Alexa Fluor® Red Fluorescent Control, Thermo Fisher Scientific, Washington, DC, USA) were used to visualize nucleic acid electrotransfer. The plasmid model used was pEGFP-N1 (4.7 kb) (Lonza, Walkersville, MD, USA), which encodes an enhanced green fluorescent protein (GFP). Plasmids were purified using Plasmid Giga Kit (Qiagen, Hilden, Germany) according to the guidelines provided by the manufacturer. The purity and concentration of pDNA were determined spectrophotometrically (Nanodrop 2000, Thermo Fisher Scientific, Washington, DC, USA).

2.3. Electroporation

Adherent cells were used for the EP experiments with oligonucleotides/siRNA and pDNA. Coverslips (Ibidi, Graefelfing, Germany) were removed from the incubator and washed twice with $1 \times$ PBS (Sigma-Aldrich, St. Louis, MO, USA). Then, the chambers were filled with EP buffer (0.1 S/m conductivity and 7.2 pH) containing 1.68 mM $MgCl_2$ (Sigma-Aldrich, St. Louis, MO, USA), 5.42 mM Na_2HPO_4 (Sigma-Aldrich, St. Louis, MO, USA), 2.91 mM NaH_2PO_4 (Sigma-Aldrich, St. Louis, MO, USA) and 270 mM sucrose (Sigma-Aldrich, St. Louis, MO, USA). The final concentration of oligonucleotides or siRNA was kept constant at 100 nM (1.29 and 1.41 μg/ml, respectively) in all experiments. The final concentrations of pDNA were set to 10, 50, and 100 μg/ml (3.2, 16.1, and 32.3 nM, respectively). In all experiments, the final volume in each chamber was 500 μl. To maintain similar conditions the following procedure was applied to each chamber separately immediately before the experiments. The time required to complete the preparation in a single chamber was approximately 10 min (5 min for sample preparation and focusing and an additional 5 min for the microscopy). Consequently, cells in the fourth chamber were outside the incubator for a maximum of 30 min before the experiment.

The cells were subjected to an electric field using custom-made aluminium electrodes (18.8 mm x 2.7 mm) positioned parallel to each other with a 3 mm spacing. These electrodes were inserted into the chamber, ensuring their placement at the bottom of the coverslip, and were connected to the pulse generator (BetaTech Electro cell B10 HV-LV, France). In this electrode configuration, the electric field was determined as the voltage-to-distance ratio. The applied voltage across the electrodes was either 240 V, resulting in an electric field of 800 V/cm, or 180 V, corresponding to an electric field of 600 V/cm.

To optimize protocols for EP, experiments were first performed with cells in suspension using the fluorescent marker propidium iodide (PI) (Sigma-Aldrich, Saint Louis, MO, USA). The concentration of cells was kept constant at 2×10^6 cells/ml. 5 μl of PI (400 μM final concentration) was added to the 45 μl of cell mixture in EP buffer either before or 15 min after electroporation and subjected to flow cytometric analysis. Experiments were performed using the electroporation cuvette with a 2 mm gap in between and two sets of EP parameters: i) 600 V/cm electric field strength, 10 ms pulse duration, and ii) 800 V/cm electric field strength, 1 ms pulse duration using a single square pulse in both cases.

2.4. Flow cytometry

The BD Accuri C6 flow cytometer (BD Biosciences, Franklin Lakes, NJ, USA) was used to perform the cytometric analysis. A flow rate of 66 μl min^{-1} was used to analyze 1×10^4 cells for each experimental point. The FL-2 emission filter was used with excitation at 488 nm and emission at 585/40 nm to evaluate the efficiency of PI electrotransfer.

2.5. Confocal fluorescence microscopy

To track the electrotransfer of molecules, experiments were performed using an inverted confocal laser scanning microscope (ZEISS LSM 710, Carl Zeiss AG, Jena, Germany). An argon laser (488 nm, 10 %
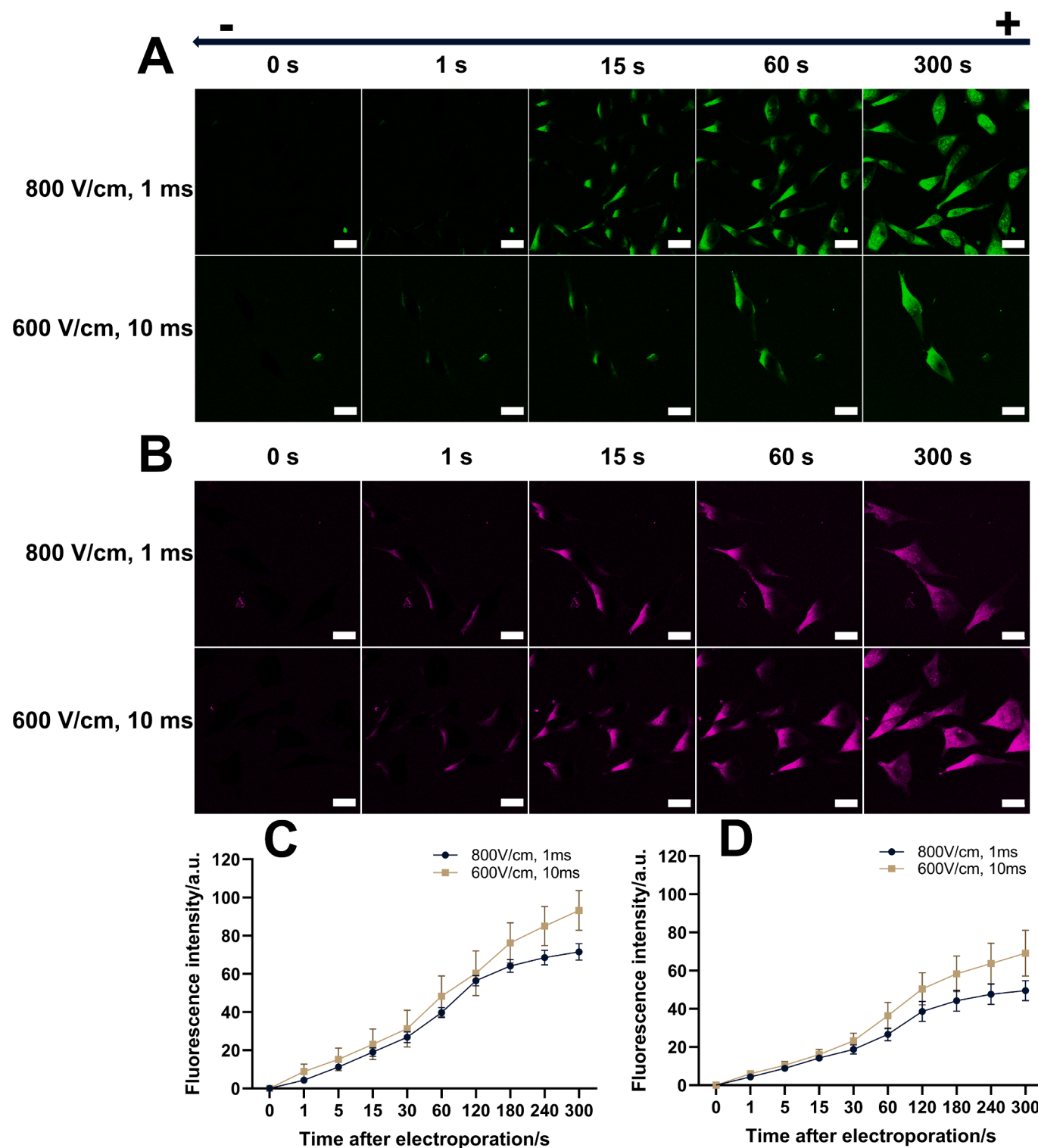
Fig. 1. Electrotransfer of oligonucleotides (A) and siRNA (B) in dependence of time after EP. Molecules were added before the application of the electric field and the uptake was monitored from up to 10 s before to 300 s after EP. Intracellular fluorescence intensity was measured within the same ROI at different time points after the electrotransfer of oligonucleotides (C) and siRNA (D). Scale bar = 20 μm. Error bars represent the standard error of the mean (SEM) of ≥ 3 independent experiments (n $\geq$ 15 cells).

laser power) was used for the excitation of oligonucleotides labeled with Alexa 488, whereas an argon laser (514 nm, 10 % laser power) – for siRNA labeled with Alexa 555. The settings were kept constant for all experimental samples. Images were acquired using a 40× (1.3 oil M27,

Carl Zeiss AG, Jena, Germany) immersion objective. The scanning speed of the laser was set to achieve a pixel dwell time of 3.15 μs. Images with 16-bit pixel depth were acquired in 512 × 512 pixel format, i.e., 153.9 × 153.9 μm.

2.6. Data analysis

The obtained images were processed using the open-source image processing software ImageJ (National Institute of Health, Bethesda, MD, USA). The fluorescence intensity of cells was measured at different time points after the application of an electric field in the same region of interest (ROI). Background fluorescence intensity (before EP) was then subtracted from the values obtained in ROI. The primary criterion for defining the ROI was the spatial distribution of cells concerning the position of the electrodes. Only cells positioned between the electrodes, displaying morphological healthy cell's shape, and maintaining no contact with each other were considered for the analysis. The presented data were obtained from at least 3 separate experiments. The entry side of oligonucleotides/siRNA was determined by measuring the fluorescence intensity distribution between the side of the cell facing the cathode or anode. To investigate the pattern of the formation of siRNA aggregates on the cell membrane in the presence of pDNA, a line encompassing approximately 1 μm of cytoplasm and an equivalent size of the extracellular milieu of the cell membrane, oriented towards the cathode (where these clusters were anticipated), was drawn. The fluorescence intensity values within this line were integrated and presented as average values. Statistical analysis and plots were generated using GraphPad Prism12.5 software. Results are presented as mean ± standard error of the mean (SEM). The statistical significance of differences between groups was determined using Mann-Whitney test. The p values < 0.05 were considered statistically significant.

3. Results

3.1. Continuous uptake of oligonucleotides and siRNA after cell electroporation

With the aim to evaluate the efficiency of the electrotransfer of oligonucleotides and siRNA, we first pre-optimized the parameters of the electric field by evaluating the intracellular delivery and cell permeabilization using PI assay and flow cytometry. The primary criteria for the selection of EP parameters were a high percentage of PI-positive cells when PI was administered prior to EP (indicating high permeability of the membrane) and a low percentage of PI-positive cells, when PI was administered after EP (indicating low irreversible permeabilization or cell death), respectively. In addition, since electrophoretic drag has been shown to be the driving force for the electrotransfer of oligonucleotides/ siRNA [29], relatively long pulses with a duration of 1–10 ms were selected. As presented in Supplemental Fig. 1, a single pulse of both sets of EP parameters 800 V/cm, 1 ms and 600 V/cm, 10 ms resulted in ≥ 95 % of permeabilized cells that were able to restore plasma membrane barrier function within 15 min after treatment.

The uptake of Alexa–488-labeled oligonucleotides and Alexa-555-labeled siRNA into cells was determined separately by acquiring confocal images before EP to 300 s after EP. The efficiency of transfer was then assessed by measuring intracellular fluorescence intensity within the same ROI at different time points after the application of the electric field.

No interaction of the oligonucleotides (Fig. 1A) or siRNA (Fig. 1B) with the cell membrane or internalization of the molecules into the cells was observed before the application of the electric field (0 s). An increase in fluorescence at the regions of the cell membrane facing the electrode plates was observed immediately after the electrical pulse of 800 V/cm, 1 ms, or 600 V/cm, 10 ms was applied. This indicates that cells were successfully permeabilized and the influx of molecules was induced by the electric field. Despite the current mechanism stating that the electrotransfer of oligonucleotides or siRNA is mainly facilitated by electrophoresis, the uptake of both molecules continued after the application of the pulse.

As can be seen in Movies S1 and S2, the fluorescent signal immediately after EP was mainly observed in the close vicinity of the cell membrane. Within 5 min, there was a shift of the fluorescence signal towards the center of the cell, followed by uniform intracellular distribution and markedly increased intracellular fluorescence. The influx of molecules after EP was also confirmed by quantitative evaluation of fluorescence intensity, presented in Fig. 1C and Fig. 1D. Before the application of the electric field, the baseline fluorescence of the cell was zero. Immediately after the application of electric field, the level of intracellular fluorescence increased to 4.4 a.u. (800 V/cm) and 8.8 A.U (600 V/cm) after oligonucleotide and 4.3 a.u. (800 V/cm) and 6-a.u. (600 V/cm) after siRNA electrotransfer, respectively. At each fixed time point, the electric field with a strength of 600 V/cm and a pulse length of 10 ms resulted in a slightly higher electrotransfer efficiency for both molecules. The intracellular fluorescence additionally increased to ~ 36.5 a.u. and 48 a.u. after oligonucleotide and siRNA electrotransfer, respectively, 60 s after treatment. A progressive increase in fluorescence was consistently noted throughout the entire observation period. Notably, at the end of the observation (300 s), there was a 2-fold increase in fluorescence as compared to the measurement taken 60 s post-pulsation.

3.2. Diffusion is more efficient through the cathode-facing side of the membrane

Consistent with the observed influx of molecules after pulsation, we also noted a fluorescence signal on both the cathode- and anode-oriented sides of the cell. To verify this observation the cells were divided in half (see Fig. S2), and the fluorescence intensity was measured on the opposite sides of the cells facing the electrodes. Measurements performed after the electrotransfer of oligonucleotides and siRNA showed a similar overall trend. The fluorescence signal appeared immediately after the application of the electric field, followed by an increase in fluorescence intensity until 120 s after treatment on both the cathode and anode sides of the cell. Although there was a significantly higher (p < 0.01) uptake and subsequent fluorescence intensity on the cathode side, there was also a substantial increase in the signal on the anode side. At 120 s, fluorescence intensity had increased to 71.4 a.u. on the cathode side and 17.4 a.u. on the anode after the electrotransfer of oligonucleotides (Fig. 2A).

When the uptake of molecules on opposite sides of the cell was evaluated, it was found that siRNA resulted in a 7.8-fold (61 a.u.) and 13.2 -fold (11 a.u.) increase in intracellular fluorescence intensity on the cathode and anode sides, respectively (compared with values obtained 1 s after the application of the electric field) (Fig. 2E). This bidirectional mode of entry (n ≥ 30 cells) was detected in ≥ 95 % (oligonucleotides) and ≥ 92 % (siRNA) of the cells examined. No cells were observed in which the molecules entered exclusively from the anode side, as shown in Fig. 2B and Fig. 2F. We also decided to evaluate the intracellular fluorescence distribution over time at a single-cell level. To do this, we drew a line delineating the position of the cell with respect to the electrodes (see Fig. S2 panels 3).

As shown previously, the fluorescence pattern after the electrotransfer of oligonucleotides (Fig. 2C and Fig. 2D) and siRNA (Fig. 2G and Fig. 2H) showed a gradual increase in intensity with time after electroporation. In particular, the fluorescence peak on the cathode side was detected 60–120 s after treatment, and a subsequent shift in fluorescence was observed, indicating the intracellular distribution of the molecules. Despite the distribution of the molecules within the cell, the signal intensity on the sides of the cell facing both the cathode and anode remained relatively constant throughout the remaining period of the observation. This indicates that the molecules continue to enter on both sides of the electroporated membrane.

3.3. Oligonucleotides and siRNA enter the nucleus

We have also detected the entry of both molecules to the nucleus of cells after the application of an electric field. To confirm that the
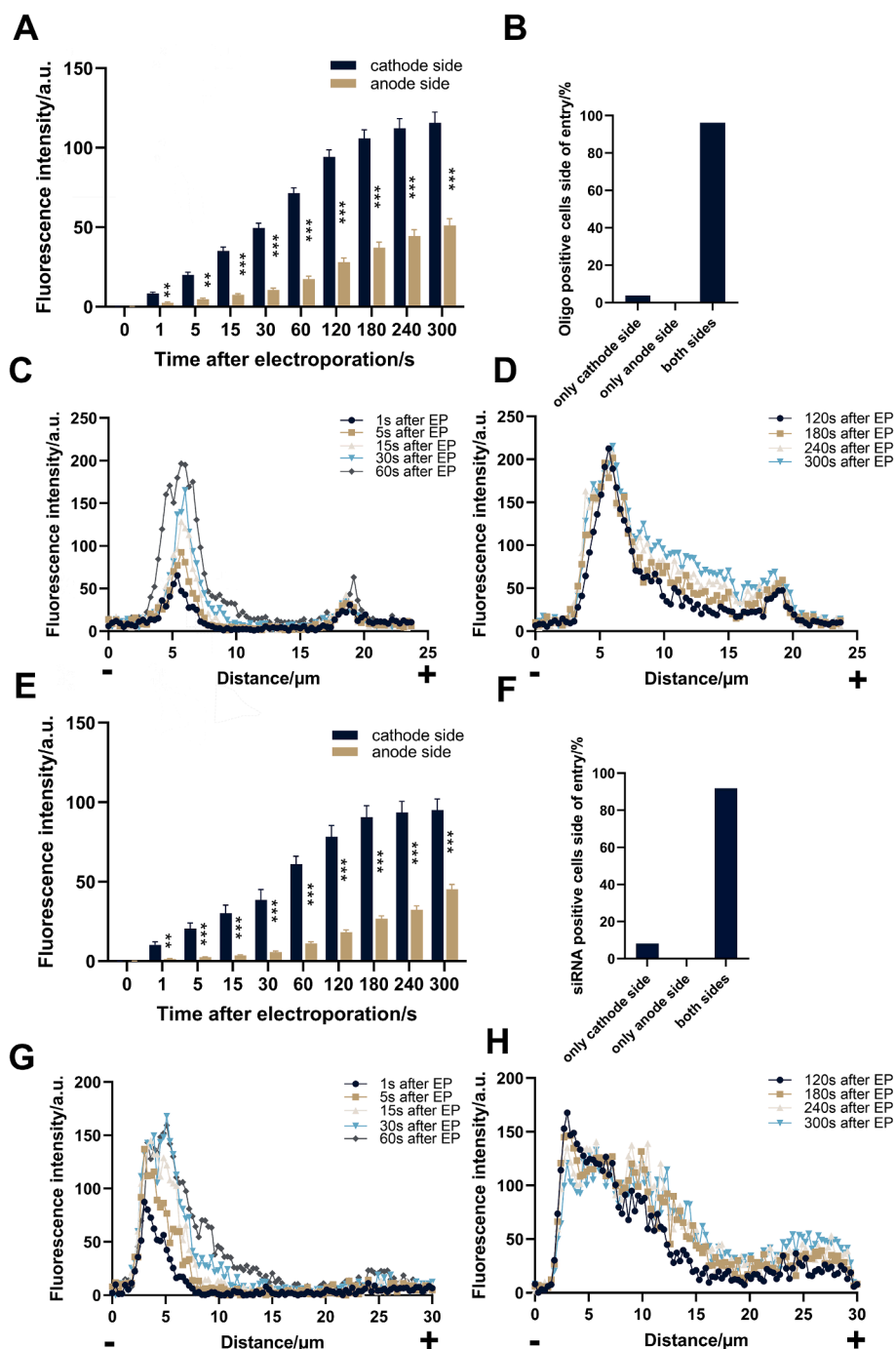
Fig. 2. Evaluation of uptake of molecules at opposite sides of the cell. Separate fluorescence intensity on the cathode- and anode-oriented side of the cell in dependence of time after the electrotransfer of oligonucleotides (A) and siRNA (E). Fluorescence intensity was measured within the same ROI. Error bars represent the standard error of the mean (SEM) of ≥ 3 independent experiments (n ≥ 20 cells). The percentage of cells taking up oligonucleotides (B) and siRNA (F) through the plasma membrane facing the cathode, anode, or both electrodes. The distribution of intracellular fluorescence of oligonucleotides (C, E, D) and siRNA (G, H) at the single cell level after the application of the electric field. Statistical differences in fluorescence intensity between the cathode and anode-oriented sides of the cell at each specified time point are indicated by *. ** denotes a p < 0.01; *** - p < 0.001.

observed signal originated from the intra-nuclear region, Z-stack images were acquired 5 min after EP. As illustrated in the representative image after the electrotransfer of oligonucleotides using an electroporation protocol of 600 V/cm electric field strength and 10 ms pulse duration (Fig. 3A and Movie S3), the molecules were homogeneously distributed in both the cytoplasm and nucleoplasm with the maximal accumulation observed in the nucleolus. The ability to cross the nuclear membrane was detected in ≥ 94 % and ≥ 91 % of cells after the electrotransfer of oligonucleotides and siRNA, respectively (Fig. 3B). To investigate the

kinetics of nuclear entry, we have also quantified the intensity of intra-nuclear fluorescence at different time points after the treatment (Fig. 3C). The appearance of a signal in the nucleus was detected as early as 5 s after EP and increased progressively for both molecules. The first significant (18.4 a.u., p < 0.001) increase as compared to 1 s after pulse application was detected 60 s after EP, coinciding with the observation of the intracellular distribution of the molecules, as described in Fig. 2. The highest intra-nuclear fluorescence intensity was observed at the end of the observation period and was ~ 65.4 a.u. and 48.7 a.u.,
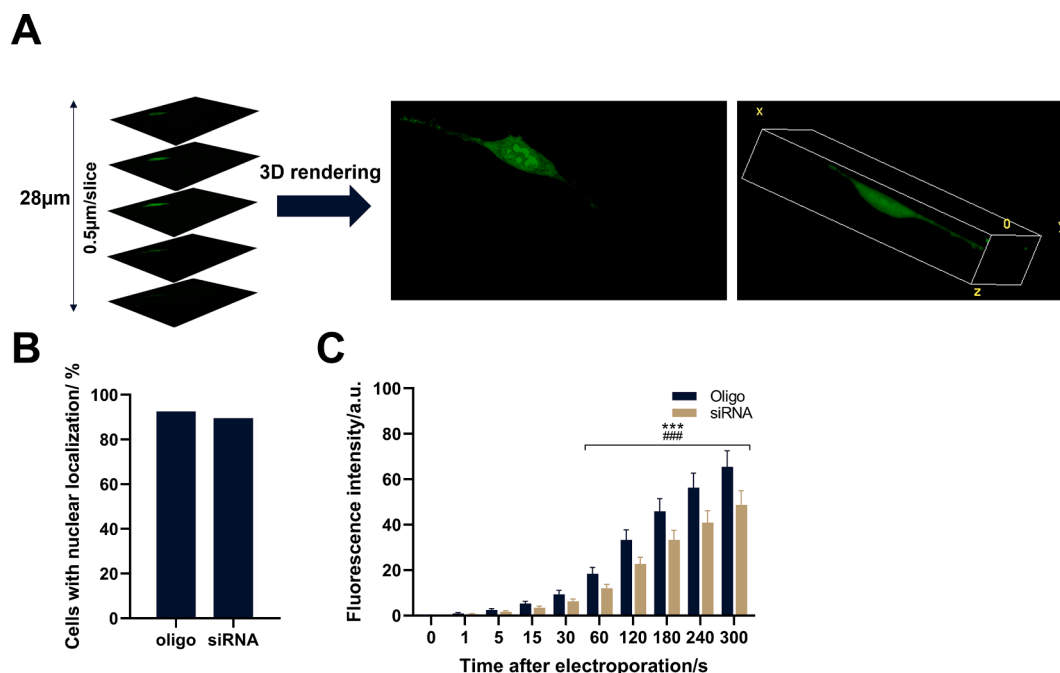
Fig. 3. Determination of intra-nuclear localization of molecules. Confocal Z-stack images were acquired in a total interval of 28 μm and rendered for a 3D reconstitution of the cell, showing nucleolar localization (A). Electric field parameters: 600 V/cm strength, 10 ms pulse duration. Images were acquired 5 min after the electrotransfer of oligonucleotides. Scale bar = 20 μm. The percentage of cells showing nuclear localization after oligonucleotide/siRNA electrotransfer (n ≥ 30) (B). Quantitative analysis of the fluorescence intensity of the nucleus at different time points after electroporation (C). Statistical differences in nucleus fluorescence intensity as compared to 1 s after pulse application are denoted by *** (for oligonucleotides) and ### (for siRNA) (p < 0.001).

respectively, after electrotransfer of oligonucleotides or siRNA (p < 0.001). These results indicate that both types of molecules are continuously taken up into the nucleus over time.

3.4. pDNA inhibits the electrotransfer of siRNA

The subsequent part of the study was to evaluate the potential influence of plasmid DNA on the EP-mediated uptake of molecules. Because i) the EP protocol of 600 V/cm electric field strength and 10 ms pulse duration resulted in more effective electrotransfer of molecules

and ii) both oligonucleotides and siRNA showed a similar pattern of cellular uptake, the experiments were conducted using only this set of EP parameters and siRNA molecules. As illustrated in Fig. 4A, the presence of pDNA during EP resulted in a gradual concentration-dependent decrease of siRNA influx. The differences in intracellular fluorescence were also confirmed by quantitative analysis, as presented in Fig. 4B. The results showed that even a low concentration of pDNA had a relevant effect on the influx of siRNA. When measured 300 s after treatment, 10 μg/ml pDNA resulted in a cellular fluorescence of 63.1 a.u. as compared with 0 μg/ml at 1 s after EP which was responsible for a 69.1
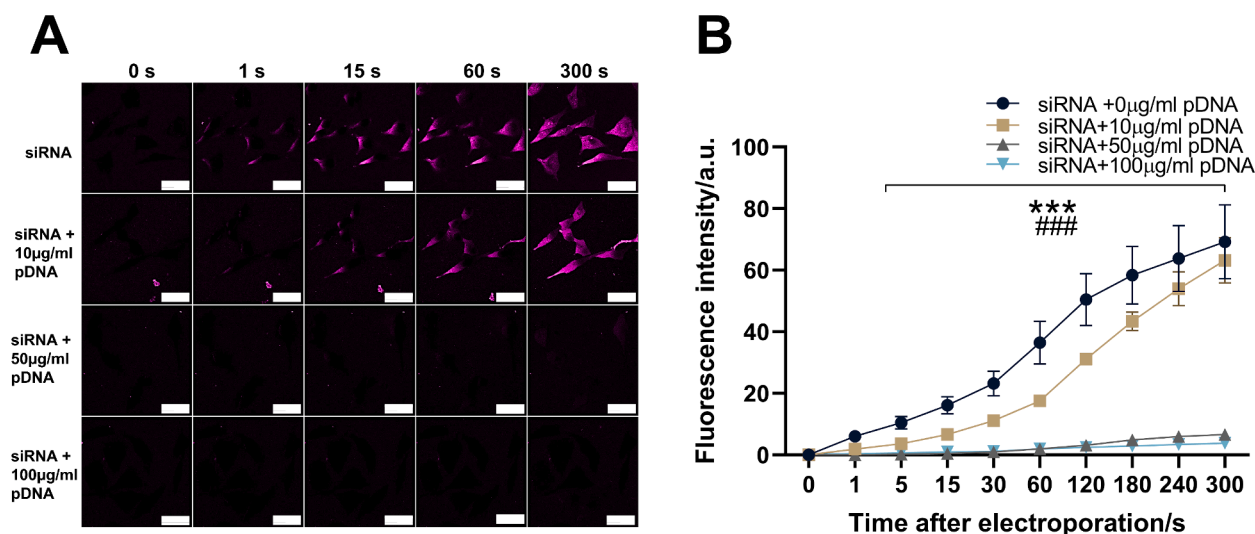

Fig. 4. The influence of pDNA on the electrotransfer efficiency of siRNA. Representative images of the variations in the intensity of intracellular fluorescence at different time points after combined electrotransfer of siRNA and pDNA (A). Experiments were performed using an electric field of 600 V/cm strength and 10 ms pulse duration. Both siRNA and pDNA molecules were administered to samples before EP. Quantitative evaluation of the dependence of fluorescence intensity on the concentration of pDNA in the samples (B). Fluorescence intensity was evaluated within the same ROI. Error bars represent the standard error of the mean (SEM) of ≥ 3 independent experiments (n ≥ 15 cells). Statistical differences between 0 and 50 or 100 μg/ml of pDNA are denoted by * and # (p < 0.001), respectively.

-a.u. fluorescence intensity. It is noteworthy that a slowed rate of uptake was observed immediately after the application of an electric pulse and persisted throughout the duration of monitoring. For example, a ~ 2-fold lower rate of uptake was observed at 60 s after treatment when 10 μg/ml of pDNA was present during EP, as opposed to the scenario where no pDNA was present in the sample. A further increase in pDNA concentration (50–100 μg/ml) resulted in a significant decrease in uptake ($p < 0.001$) of the molecules: intracellular fluorescence increased only to 6.6 a.u. and 3.8 a.u. at 50 μg/ml and 100 μg/ml pDNA, respectively (300 s after treatment).

3.5. pDNA induces the formation of siRNA clusters

In addition to significantly reduced intracellular fluorescence intensity, accumulation of siRNA was observed exclusively on the cell side facing the cathode. At a low pDNA concentration (10 μg/ml) limited number of these fluorescent clusters were noticed and they were no longer perceptible at the end of the observation period. Clusters were not observed when no pDNA was present in the sample. At pDNA levels greater than 50 μg/ml, the number of clusters increased significantly, and they remained localized on the plasma membrane throughout the 5-min period. This was also accompanied by delayed translocation of siRNA molecules across the plasma membrane. To gain a better understanding of the observed decreased cellular uptake and siRNA cluster formation, we quantified the fluorescence intensity at the cell membrane

facing the cathode immediately after pulse application. The principle of the measurements and the results obtained are shown in Fig. 5A and Fig. 5B (pDNA concentration ≤ 10 μg/ml) as well as Fig. 5C and Fig. 5D (pDNA concentration ≥ 50 μg/ml). The results show that without pDNA (0 μg/ml) in the sample, translocation of siRNA molecules across the plasma membrane occurs in a fairly uniform manner. Fluorescence remained constant throughout the membrane at a level of ≥ 17.5 a.u., with a peak maximum of 32.2 a.u. Comparable and uniform uptake of siRNA was observed in the presence of 10 μg/ml pDNA, albeit with lower fluorescence intensity, with a maximum peak of 18.9 a.u. Consistent with the observed formation of clusters, the presence of multiple fluorescence peaks with significantly different intensities was observed at the cell membrane upon increasing pDNA concentration to 50–100 μg/ml. Despite the similarity of fluorescence variations observed in both cases, increasing the concentration of pDNA resulted in a greater number of fluorescence peaks.

3.6. The electrotransfer of siRNA is hindered by the aggregation of nucleic acids

We also found that the uptake of siRNA on the side facing the anode was no longer observed when the concentration of plasmid DNA exceeded 50 μg/ml. To confirm this finding, we again divided the cell with respect to the position of the electrodes, as shown in Fig. S3, and measured the fluorescence intensity on both sides separately (Fig. 6 A-
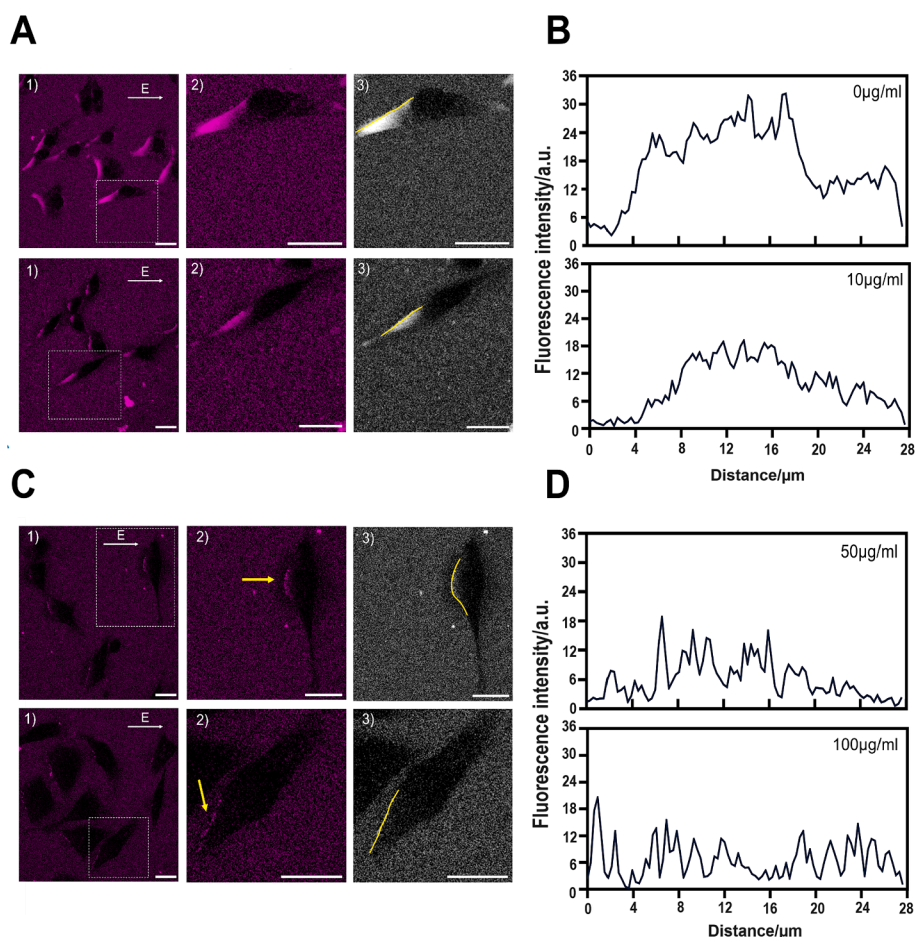

Fig. 5. Evidence of siRNA cluster formation on the cathode-oriented side of the cell. The plots show the fluorescence intensity patterns on the cathode-facing side of the cell membrane when 0–10 μg/ml (B) and 50–100 μg/ml (D) of pDNA were present during electroporation. The strategy of measuring clustered area (A, C): 1) images 1 s after EP. Cells marked with a dashed square were used for the analysis; 2) yellow arrows mark the siRNA clusters; 3) lines encompassing ~ 1 μm of cytoplasm and an equivalent size of the extracellular milieu were traced. Intensities between these distances were integrated and presented as the average values. Experiments were performed using an electric field of 600 V/cm strength and 10 ms pulse duration. Both siRNA and pDNA molecules were administered to the samples before the application of the electric field. Scale bar = 20 μm.
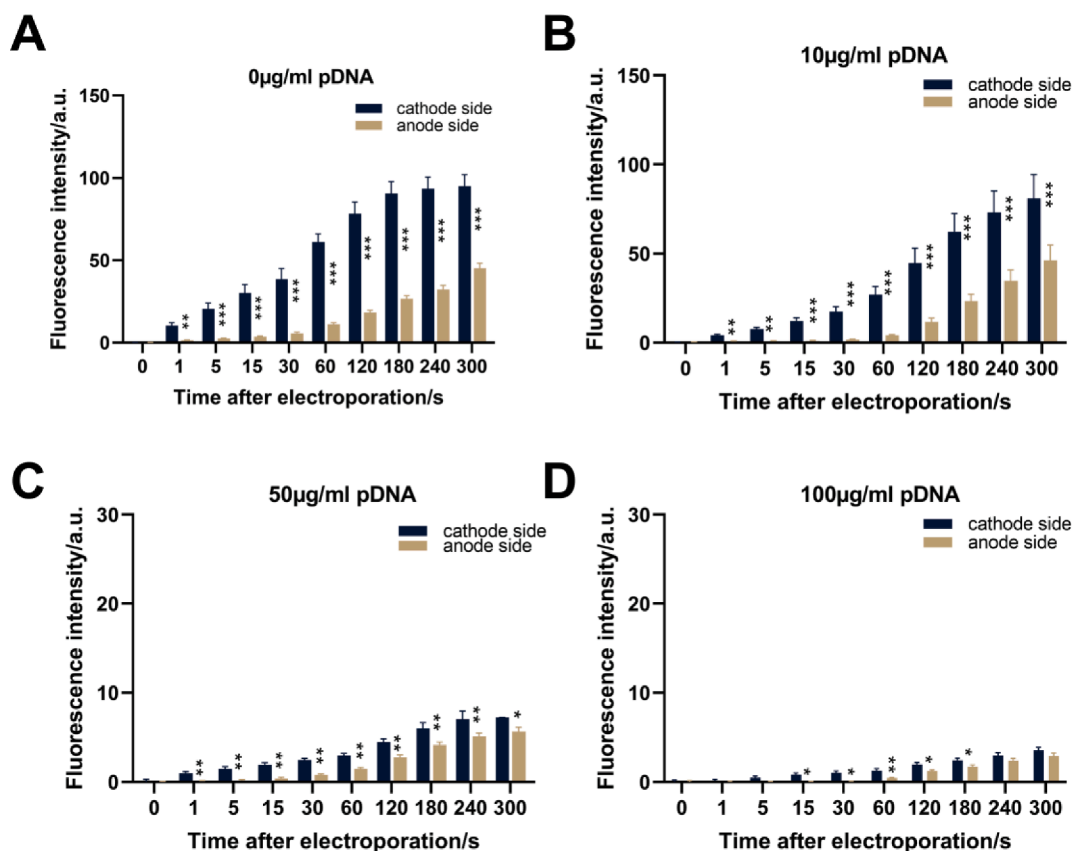
Fig. 6. The dynamics of fluorescence intensity on the cathode and anode side of the cells after EP with 0 μg/ml (A), 10 μg/ml (B), 50 μg/ml (C) and 100 μg/ml (D) of pDNA. Fluorescence intensity was measured within the same ROI. Error bars represent the standard error of the mean (SEM) of ≥ 3 independent experiments ($n \geq 15$ cells). Statistical differences in fluorescence intensity between the cathode and anode-oriented sides of the cell at each specified time point are indicated by *. * denotes a $p < 0.05$; ** - $p < 0.01$; *** - $p < 0.001$.

D). The results confirmed a decrease in the uptake of molecules on both the cathode- and anode-oriented sides of the cell that was dependent on pDNA concentration. Quantified 300 s after treatment, uptake on the cathode side was 1.1-fold (81.1 a.u.), 13.2-fold (7.2 a.u.), and 27.14-fold (3.5 a.u.) lower ($p < 0.05$), when 10, 50, and 100 μg/ml of pDNA were present, respectively in comparison to no pDNA in the sample (95 a.u.). Interestingly, the influx of siRNA at the anode side was also 8fold (5.6 a. u.) lower at 50 μg/ml pDNA and almost 15.6-fold (2.9 a.u.) lower at 100 μg/ml than at 0 μg/ml DNA (45.2 a.u.) ($p < 0.05$). These results suggest that the negative effect of pDNA on siRNA electrotransfer is not solely due to the formation of clusters.

4. Discussion

Although RNAi is a powerful and rapidly developing technology that allows precise regulation of target gene activity, its application is limited due to the insufficient efficiency of the delivery of nucleic acids. Therefore, understanding the basic principles that govern the cellular uptake of molecules could potentially improve the efficiency of the treatment. In this study, we have examined EP-mediated delivery of oligonucleotides and siRNA at the single-cell level. In addition, we investigated the influence of large nucleic acid (pDNA) on the efficiency of the electrotransfer of small nucleic acids. By observing the uptake of oligonucleotides and siRNA over a 5-min period, we demonstrated that the influx of these molecules after cell EP continued throughout the whole observation period (Fig. 1A and Fig. 1B, Movies S1 and S2). The fact that no aggregate formation was observed at the cell membrane supports the assumption that the molecules have direct access to the cytoplasm during the process. This suggests that at least for the molecule size used in this study (35 nt long single-stranded DNA oligonucleotide

and ~ 21 bp double-stranded siRNA), both exhibit comparable uptake patterns of small charged molecules, such as PI, that enter the cell by diffusion. Moreover, electrophoresis can only occur in the presence of an electric field, which does not explain the observed gradual increase in fluorescence intensity over time (Fig. 1C and Fig. 1D) and the bidirectional entry of both molecules (Fig. 2). Therefore, the obtained results (Fig. 2) indicate that the influx of both molecules is the consequence of the interaction of electrophoretic force and post-pulsation diffusion.

Until now, the prevailing theory was that the direct transfer of siRNA across the plasma membrane into the cell cytoplasm occurs exclusively on the side facing the cathode [29]. According to the authors, even though the electroporated membrane allows for continuous PI uptake driven by an electrochemical gradient, no free diffusion of siRNA molecules occurs at the same EP conditions, and the molecules enter the cytoplasm only during electric pulses. Therefore, the current concept emphasizes the crucial importance of electrophoretic forces. Similarly, Lojk et al. (2015) reported a strong dependence of siRNA-induced silencing on pulse strength and pulse duration, even for EP parameters that resulted in nearly 100 % permeabilization [47]. In this study, we observed a similar phenomenon – the exposure of cells to a 600 V/cm strength and 10 ms long electric pulse compared to 800 V/cm and 1 ms pulse resulted in increased electrotransfer efficiency for both molecules, although the levels of membrane permeabilization were comparable for PI (see Supplemental Fig. 1). However, regardless of the EP protocols applied, the intensity of intracellular fluorescence was observed to be higher after a longer period (minutes) after EP, than immediately after the delivery of the electrical pulse, suggesting that diffusion plays a significant role in the transfer of oligonucleotides and siRNA. The fact that both molecules can enter the cell continuously from both the cathode and anode sides also supports this assumption. On the other
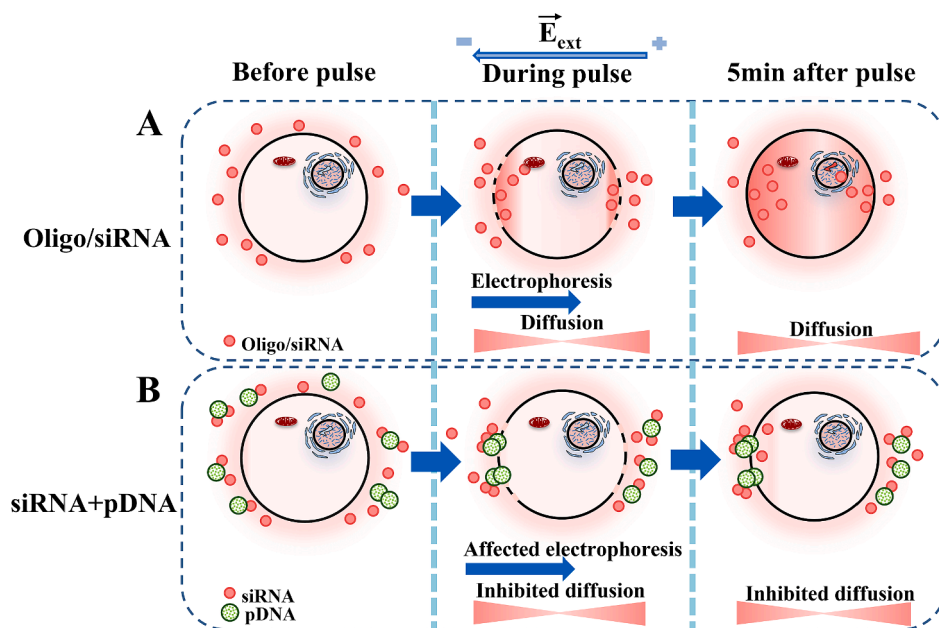
Scheme 1. An updated mechanism of electrotransfer of oligonucleotides/siRNA (a) and a new suggested model of cellular uptake of siRNA after simultaneous electrotransfer with pDNA (b). Oligonucleotides and siRNA employ a common mechanism of cellular uptake. The delivery commences promptly following the application of an electric pulse and continues for several minutes thereafter. The entrance of molecules involves both electrophoresis (during the pulse) and diffusion (during and after the pulse). The uptake is present on both the cathode and anode sides of the cell, with a notable preference for the cathodal side. Within minutes of the electric pulse, oligonucleotides, and siRNA cross the nucleus and accumulate within the nucleoli. The presence of pDNA during the electrotransfer of siRNA obstructs the passage of siRNA molecules, leading to the formation of siRNA clusters specifically on the side of the cell oriented towards the cathode. Additionally, pDNA has the potential to aggregate with multiple siRNA molecules and negatively affect electrophoresis on the cathode side and inhibit diffusion of siRNA on both the cathode and anode sides of the cell.

hand, the significant cathodic preference exhibited by both oligonucleotides and siRNA upon entering the cell (Fig. 2 C, D, G, H) shows important differences from the uptake pattern of small molecules. The most obvious hypothesis to explain higher uptake at the cathode side might be the influence of electrophoretic forces. These forces facilitate the movement of oligonucleotides and siRNA toward the cathode-facing membrane and allow them to move directly through the electroporated membrane during the pulse by overcoming electrostatic repulsion. In addition, electrophoretic movement presumably increases the number of molecules in close proximity to the cathode-facing side of the cell, causing the asymmetry of the uptake to persist after the end of the electric pulse. Finally, the level of EP could be more favorable in terms of the area of the electroporated membrane and/or the size of the electropores on the membrane facing the cathode. Indeed, studies have shown that the asymmetry with a cathodic preference for ion and dye uptake was observed after EP [48–51]. A similar pattern was also observed after siRNA electrotransfer in 3D spheroids [15].

Our results also show that oligonucleotides/siRNA can enter the nucleus within minutes after electroporation (Fig. 3A and Fig. 3B). Indeed, the transfer of single-stranded LNA/DNA oligomers (~7 kDa) to the nucleus after EP has been already reported [30]. Previous studies have also shown that the intracellular localization of siRNA and oligonucleotides is not restricted to the cytoplasm and both molecules are able to cross the nuclear membrane [30,52]. In a study performed by Jarve et al. [52], siRNA was detected in the nucleus within 15 min after microinjection into the cytoplasm. 4 h later, siRNA had completely migrated back into the cytoplasm. In another study, intra-nuclear localization of siRNA was detected as early as 2 min after microinjection [53]. This bidirectional exchange between the nucleus and cytoplasm is thought to be facilitated by nuclear pore complexes (NPCs). NPC channels allow passive diffusion of molecules having a molecular mass lower than 40 kDa [54]. Exportin 5 is assumed to be responsible for the regulation of siRNA transfer from the nucleus [55]. Of note, significant amounts of Ago2, a catalytic driver of RNA interference, have also

been detected in the nucleus [56,57]. Therefore, the evidence, that NPCs are in sufficient size to allow the free diffusion of oligonucleotides/siRNA, and, that RNA interference can function within the nucleus, collectively account for the rapid movement of the molecules to the nucleoplasm. In agreement, we observed a significant accumulation of siRNA and oligonucleotide molecules in the nucleus within 1 to 2 min after treatment, which coincided with the widespread distribution of the molecules within the cell. This observation suggests that the transport of the molecules to the nucleus occurred upon their reach of the nuclear membrane. This may explain the faster kinetics of nuclear localization observed after EP compared with microinjection. Studies have also suggested that fluorescently labeled siRNA is excluded from non-nucleolar regions after the entry into the nucleus and accumulates significantly in the nucleoli [55,58], a similar pattern was also observed in our study. The physiological significance of this specific accumulation pattern, however, is not yet clearly understood.

This study introduces an updated electrotransfer mechanism for oligonucleotides/siRNA, proposed previously by Paganin-Gioanni et al. [29]. The authors of the study employed a distinct cell line and electric field parameters. Although B16 F10 and CHO cells share similar diameters, the CHO cells used in our study exhibited elongated shapes, as evident in the provided images. Furthermore, the authors reported a fluorescence signal on the cathode side exceeding 200 a.u. after applying a series of 10 pulses. In contrast, our study revealed a comparable signal only minutes post-pulse application, which did not show further increase over time, but rather exhibited uniform distribution within the cell (refer to Fig. 3D and Fig. 3H). It is noteworthy that the authors utilized approximately three times lower siRNA concentration compared with our study, with initial amounts of 4 μg and 14.1 μg, respectively. This implies a substantially higher cumulative electrophoretic force when employing parameters 10 pulses of 300 V/cm, 5 ms, resulting in a more significant influx of molecules during the pulsation. Presumably, this high fluorescence signal could hinder a clear discrimination of post-pulse diffusion of labeled siRNA molecules, while still

detecting siRNA-induced silencing of EGFP mRNA. Additionally, the authors monitored siRNA electrotransfer for up to one minute. Consistent with our findings, nuclear localization of molecules was not observed within the first minute after electroporation. Consequently, the cytoplasmic localization of siRNA reported by the authors may be attributed to the limited observation timeframe.

In this study, we demonstrated for the first time that the presence of pDNA during the electroporation significantly reduces the delivery of small fluorescently labeled nucleic acids (Fig. 4). It is well known that the electrotransfer of pDNA is driven by electrophoresis and the entry of the molecules occurs at the cathode side of the cell [36–39,59,60]. Since results revealed that the cathode side is the preferred site for the electrotransfer of siRNA, it is conceivable that pDNA impedes the entry of much smaller siRNA molecules. Since pDNA remains in contact with the cell membrane for several minutes after EP [60,61] the diffusion of siRNA molecules would be hindered or significantly reduced after the pulsation at the cathode side, making the anode side the primary entry point. Therefore, the observed decrease in molecular influx could be partially explained by the uptake exclusively occurring on the anode side. Consistent with the notion of membrane obstruction on the cathode side, we observed the formation of siRNA clusters at the membrane in the presence of pDNA during the treatment (Fig. 5). Previous studies have shown that DNA does not distribute uniformly across the membrane before translocation to the cytoplasm, but forms discrete aggregates after application of an electrical pulse [61]. Consequently, it could be hypothesized that a higher concentration of pDNA would involve a larger number of molecules, resulting in a greater amount of DNA aggregates at the membrane. This could explain the increasing number of siRNA clusters with increasing pDNA concentration, as observed in our study. Nevertheless, the formation of clusters alone cannot explain the significantly decreased uptake of siRNA on the cell side facing the anode, as shown in Fig. 6.

Previous research by Kooimans et al. [62] suggests that EP can stimulate the strong aggregation of siRNA molecules due to precipitation, induced by metal ions from the electrodes, hydroxyl and oxide ions generated during electric pulsing and hydroxide ions from the EP medium. Similarly, ion-induced pDNA aggregation was observed after EP in another study [63]. It was suggested that positively charged metal ions from the electrodes may interact with negatively charged residues of nucleic acids, neutralizing the repulsive forces between macromolecules or even forming metal bridges between them and, in turn, facilitating the formation of aggregates. Meanwhile, the interaction between hydroxyl and oxide ions with metal ions can lead to the formation of substantial aggregates. These aggregates, in turn, have the potential to induce the aggregation of pDNA during the electrotransfer [64]. The presence of divalent cations (e.g., Mg^{2+}) in the EP buffer is also associated with the neutralization of the charges of nucleic acids and subsequent aggregation [65,66]. Although we did not observe any difference in the efficiency of siRNA electrotransfer when using stainless steel or aluminum electrodes (data not shown), we cannot rule out the possibility that larger pDNA molecules could aggregate with multiple siRNA molecules, physically reducing the number of free siRNA molecules. Conversely, the appearance of fluorescent structures on the membrane side facing the cathode during siRNA electrotransfer in the presence of pDNA suggests that these structures correspond to siRNA/pDNA aggregates. Indeed, similar fluorescent structures were observed during the electrotransfer of fluorescently labeled pDNA [33]. Taken together, the formation of clusters on the cathode side in conjunction with the potential aggregation of pDNA and siRNA could explain the significant reduction in the cellular uptake of siRNA.

In summary, in this study, we provide an update to the conventional mechanism of cellular uptake of small nucleic acids, by revealing new fundamental insights into the mechanism of electrotransfer of oligonucleotides and siRNA (Scheme 1). Our results have demonstrated that siRNA and oligonucleotides enter the cell through: i) the side of the membrane facing the cathode due to electrophoretic forces during the

electric pulse and ii) both sides of the electroporated membrane due to diffusion after the application of the electric pulse. In addition, both molecules are transported to the nucleus within minutes after treatment, with significant accumulation in the nucleoli. We also discovered that the presence of pDNA during siRNA electrotransfer significantly reduces the efficiency of siRNA electrotransfer, presumably by blocking the passage sites at the membrane facing the cathode and by reducing free siRNA molecules due to aggregation with pDNA. Collectively, our data shed light on the independent and simultaneous electrotransfer mechanism of oligonucleotides/siRNA and pDNA, potentially offering a new perspective for the clinical development of RNAi-based therapies.

CRediT authorship contribution statement

Rūta Palepšienė: Writing – original draft, Methodology, Investigation, Formal analysis, Data curation, Conceptualization. **Aswin Muralidharan:** Writing – review & editing, Methodology, Formal analysis. **Martynas Maciulevičius:** Writing – review & editing, Methodology, Formal analysis. **Paulius Ruzgys:** Writing – review & editing, Methodology. **Sonam Chopra:** Writing – review & editing, Methodology, Investigation, Data curation. **Pouyan E. Boukany:** Writing – review & editing, Validation, Supervision, Methodology, Investigation, Formal analysis, Conceptualization. **Saulius Šatkauskas:** Writing – review & editing, Validation, Supervision, Methodology, Investigation, Funding acquisition, Formal analysis, Conceptualization.

Declaration of competing interest

The authors declare that they have no known competing financial interests or personal relationships that could have appeared to influence the work reported in this paper.

Data availability

No data was used for the research described in the article.

Acknowledgments

Appendix A. Supplementary data

Supplementary data to this article can be found online at https://doi.org/10.1016/j.bioelechem.2024.108696.

References

[1] S. Takashima, Electroporation and Electrofusion in Cell Biology. Eberhard Neumann, Arthur E. Sowers, Carol A. Jordan. Q Rev Biol. 65 (2) (1990).

[2] E. Neumann, M. Schaefer-Ridder, Y. Wang, P.H. Hofschneider, Gene transfer into mouse lyoma cells by electroporation in high electric fields, EMBO J. 1 (7) (1982) 841–845.

[3] V.A. Klenchin, S.I. Sukharev, S.M. Serov, L.V. Chernomordik, Y.A. Chizmadzhev, Electrically induced DNA uptake by cells is a fast process involving DNA electrophoresis, Biophys. J. 60 (4) (1991).

[4] S. Satkauskas, M.F. Bureau, M. Puc, A. Mahfoudi, D. Scherman, D. Miklavcic, et al., Mechanisms of in vivo DNA Electrotransfer: respective contributions of cell electropermeabilization and DNA electrophoresis, Mol. Ther. 5 (2) (2002) 133–140.

[5] S.I. Sukharev, V.A. Klenchin, S.M. Serov, L.V. Chernomordik, C. YuA, Electroporation and electrophoretic DNA transfer into cells. the effect of DNA interaction with electropores, Biophys. J. 63 (5) (1992) 1320–1327.

[6] J. Nguyen, F.C. Szoka, Nucleic acid delivery: the missing pieces of the puzzle? Acc Chem. Res. 45 (7) (2012).

[7] N. Nakai, T. Kishida, M. Shin-Ya, J. Imanishi, Y. Ueda, S. Kishimoto, et al., Therapeutic RNA interference of malignant melanoma by electrotransfer of small interfering RNA targeting mitf, Gene Ther. 14 (4) (2007).

[8] D. Navickaite, P. Ruzgys, V. Novickij, M. Jakutaviciute, M. Maciulevicius, R. Sinceviciute, et al., Extracellular-Ca2+-induced decrease in small molecule electrotransfer efficiency: Comparison between Microsecond and Nanosecond electric pulses, Pharmaceutics. 12 (5) (2020) 422.

[9] M. Casciola, M. Tarek, A molecular insight into the electro-transfer of small molecules through electropores driven by electric fields. biochimica et biophysica acta (BBA) -, Biomembranes 1858 (10) (2016) 2278–2289.

[10] S. Chabot, S. Pelofy, A. Paganin-Gioanni, J. Teissie, M. Golzio, Electrotransfer of RNAi-based oligonucleotides for oncology, Anticancer Res. 31 (2011).

[11] D. Bumcrot, M. Manoharan, V. Koteliansky, D.W.Y. Sah, RNAi therapeutics: a potential new class of pharmaceutical drugs, Nat. Chem. Biol. 2 (2006).

[12] Y. Takei, T. Nemoto, P. Mu, T. Fujishima, T. Ishimoto, Y. Hayakawa, et al., In vivo silencing of a molecular target by short interfering RNA electroporation: tumor vascularization correlates to delivery efficiency, Mol Cancer Ther. 7 (1) (2008).

[13] M. Breton, L. Delemotte, A. Silve, L.M. Mir, M. Tarek, Transport of siRNA through lipid membranes driven by nanosecond electric pulses: an experimental and computational study, J Am Chem Soc. 134 (34) (2012).

[14] C. Luft, R. Ketteler, Electroporation knows no Boundaries: the use of electrostimulation for siRNA delivery in cells and tissues, SLAS Discovery. 20 (8) (2015) 932–942.

[15] S. Pelofy, H. Bousquet, L. Gibot, M.P. Rols, M. Golzio, Transfer of small interfering RNA by electropermeabilization in tumor spheroids, Bioelectrochemistry 141 (2021) 107848.

[16] T. Matsuda, C.L. Cepko, Electroporation and RNA interference in the rodent retina *in vivo* and *in vitro*, Proc. Natl. Acad. Sci. 101 (1) (2004) 16–22.

[17] Y. Takabatake, Y. Isaka, M. Mizui, H. Kawachi, F. Shimizu, T. Ito, et al., Exploring RNA interference as a therapeutic strategy for renal disease, Gene. Ther. 12 (12) (2005) 965–973.

[18] Y. Akaneya, B. Jiang, T. Tsumoto, RNAi-induced gene silencing by local electroporation in Targeting brain region, J. Neurophysiol. 93 (1) (2005) 594–602.

[19] T. Kishida, H. Asada, S. Gojo, S. Ohashi, M. Shin-Ya, K. Yasutomi, et al., Sequence-specific gene silencing in murine muscle induced by electroporation-mediated transfer of short interfering RNA, J. Gene Med. 6 (1) (2004) 105–110.

[20] Y. Dorsett, T. Tuschl, siRNAs: applications in functional genomics and potential as therapeutics, Nat. Rev. Drug Discov. 3 (4) (2004) 318–329.

[21] H. Dana, G.M. Chalbatani, H. Mahmoodzadeh, R. Karimloo, O. Rezaiean, A. Moradzadeh, et al., Molecular mechanisms and biological functions of siRNA, Int J Biomed Sci. 13 (2) (2017) 48–57.

[22] J. Neumeier, G. Meister, siRNA specificity: RNAi mechanisms and strategies to reduce off-Target effects, Front Plant Sci. 28 (2021) 11.

[23] C.F. Bennett, E.E. Swayze, RNA Targeting therapeutics: Molecular mechanisms of antisense oligonucleotides as a therapeutic platform, Annu. Rev. Pharmacol. Toxicol. 50 (1) (2010) 259–293.

[24] Koutsilieri E, Rethwilm A, Scheller C. The therapeutic potential of siRNA in gene therapy of neurodegenerative disorders. In: Neuropsychiatric Disorders An Integrative Approach. Vienna: Springer Vienna; p. 43–9.

[25] L. Moumné, A.C. Marie, N. Crouvezier, Oligonucleotide therapeutics: from discovery and development to patentability, Pharmaceutics. 14 (2) (2022) 260.

[26] K. Takakura, A. Kawamura, Y. Torisu, S. Koido, N. Yahagi, M. Saruta, The clinical potential of oligonucleotide therapeutics against pancreatic cancer, Int. J. Mol. Sci. 20 (13) (2019) 3331.

[27] D. Di Fusco, V. Dinallo, I. Marafini, M.M. Figliuzzi, B. Romano, G. Monteleone, Antisense oligonucleotide: basic concepts and therapeutic application in inflammatory bowel disease, Front Pharmacol. 29 (2019) 10.

[28] R. Garzon, G. Marcucci, C.M. Croce, Targeting microRNAs in cancer: rationale, strategies and challenges, Nat Rev Drug Discov. 9 (10) (2010) 775–789.

[29] A. Paganin-Gioanni, E. Bellard, J.M. Escoffre, M.P. Rols, J. Teissié, M. Golzio, Direct visualization at the single-cell level of siRNA electrotransfer into cancer cells, Proc Natl Acad Sci U S a. 108 (26) (2011).

[30] S. Chabot, J. Orio, R. Castanier, E. Bellard, S.J. Nielsen, M. Golzio, et al., LNA-based oligonucleotide Electrotransfer for miRNA inhibition, Mol. Ther. 20 (8) (2012) 1590–1598.

[31] N.Y. Sardesai, D.B. Weiner, Electroporation delivery of DNA vaccines: prospects for success, Curr Opin Immunol. 23 (3) (2011) 421–429.

[32] S.H. Lee, S.N. Danishmalik, J.I. Sin, DNA vaccines, electroporation and their applications in cancer treatment, Hum Vaccin Immunother. 11 (8) (2015) 1889–1900.

[33] Golzio M, Teissié J, Rols MP. Direct visualization at the single-cell level of electrically mediated gene delivery. Proceedings of the National Academy of Sciences. 2002 Feb 5;99(3):1292–7.

[34] E. Phez, C. Faurie, M. Golzio, J. Teissié, M.P. Rols, New insights in the visualization of membrane permeabilization and DNA/membrane interaction of cells submitted to electric pulses, Biochim. Biophys. Acta Gen. Subj. 1724 (3) (2005) 248–254.

[35] S. Sachdev, T. Potočnik, L. Rems, D. Miklavčič, Revisiting the role of pulsed electric fields in overcoming the barriers to in vivo gene electrotransfer, Bioelectrochemistry Vol. 144 (2022).

[36] C. Rosazza, S. Haberl Meglic, A. Zumbusch, M.P. Rols, D. Miklavcic, Gene Electrotransfer: a mechanistic perspective, Curr Gene Ther. 16 (2) (2016) 98–129.

[37] C. Favard, D. Dean, M.P. Rols, Electrotransfer as a non viral method of gene delivery, Curr Gene Ther. 7 (1) (2007).

[38] Rols MP. Gene Delivery by electroporation in vitro: Mechanisms. In: Handbook of Electroporation. 2017.

[39] M. Pavlin, M. Kanduser, New insights into the mechanisms of gene Electrotransfer – Experimental and theoretical analysis, Sci Rep. 5 (1) (2015) 9132.

[40] E.E. Vaughan, D.A. Dean, Intracellular trafficking of plasmids during transfection is mediated by microtubules, Mol. Ther. 13 (2) (2006).

[41] V.A. Klenchin, S.I. Sukharev, S.M. Serov, L.V. Chernomordik, Y.A. Chizmadzhev, Electrically induced DNA uptake by cells is a fast process involving DNA electrophoresis, Biophys J. 60 (4) (1991) 804–811.

[42] S. Chopra, P. Ruzgys, M. Jakutaviciute, A. Rimgailaite, D. Navickaitė, S. Satkauskas, A novel method for controlled gene expression via combined bleomycin and plasmid DNA Electrotransfer, Int. J. Mol. Sci. 20 (16) (2019) 4047.

[43] P. Ruzgys, M. Jakutaviciute, S. Chopra, S. Satkauskas, Enhancement of drug electrotransfer by extracellular plasmid DNA, Arch Biochem Biophys. 666 (2019) 156–160.

[44] J.N. Søndergaard, K. Geng, C. Sommerauer, I. Atanasoai, X. Yin, C. Kutter, Successful delivery of large-size CRISPR/Cas9 vectors in hard-to-transfect human cells using small plasmids, Commun Biol. 3 (1) (2020) 319.

[45] M. Wu, F. Yuan, Membrane binding of plasmid DNA and endocytic pathways are involved in Electrotransfection of mammalian cells, PLoS One 6 (6) (2011) e20923.

[46] Y. Wang, C.C. Chang, L. Wang, F. Yuan, Enhancing cell viability and efficiency of plasmid DNA Electrotransfer through reducing plasma membrane permeabilization, Bioelectricity. 2 (3) (2020) 251–257.

[47] J. Lojk, K. Mis, S. Pirkmajer, M. Pavlin, siRNA delivery into cultured primary human myoblasts - optimization of electroporation parameters and theoretical analysis, Bioelectromagnetics 36 (8) (2015) 551–563.

[48] K. Kinosita, H. Itoh, S. Ishiwata, K. Hirano, T. Nishizaka, T. Hayakawa, Dual-view microscopy with a single camera: real-time imaging of molecular orientations and calcium, J. Cell Biol. 115 (1) (1991) 67–73.

[49] T. Batista Napotnik, D. Miklavčič, Pulse duration dependent Asymmetry in Molecular transmembrane transport due to electroporation in H9c2 rat Cardiac myoblast cells in vitro, Molecules 26 (21) (2021) 6571.

[50] Tekle E, Astumian RD, Chock PB. Selective and asymmetric molecular transport across electroporated cell membranes. Proceedings of the National Academy of Sciences. 1994 Nov 22;91(24):11512–6.

[51] E.B. Sözer, C.F. Pocetti, P.T. Vernier, Asymmetric patterns of small molecule transport after Nanosecond and Microsecond electropermeabilization, J Membr Biol. 251 (2) (2018) 197–210.

[52] A. Järve, J. Müller, I.H. Kim, K. Rohr, C. MacLean, G. Fricker, et al., Surveillance of siRNA integrity by FRET imaging, Nucleic Acids Res. 35 (18) (2007) e124.

[53] G.L. Lukacs, P. Haggie, O. Seksek, D. Lechardeur, N. Freedman, A.S. Verkman, Size-dependent DNA mobility in cytoplasm and nucleus, J. Biol. Chem. (2000) 275(3).

[54] H. Fried, U. Kutay, Nucleocytoplasmic transport: taking an inventory, Cell Mol Life Sci. 60 (8) (2003) 1659–1688.

[55] T. Ohrt, In situ fluorescence analysis demonstrates active siRNA exclusion from the nucleus by exportin 5, Nucleic Acids Res. 34 (5) (2006) 1369–1380.

[56] T. Ohrt, J. Mütze, W. Staroske, L. Weinmann, J. Höck, K. Crell, et al., Fluorescence correlation spectroscopy and fluorescence cross-correlation spectroscopy reveal the cytoplasmic origination of loaded nuclear RISC in vivo in human cells, Nucleic Acids Res. 36 (20) (2008) 6439–6449.

[57] K.T. Gagnon, L. Li, Y. Chu, B.A. Janowski, D.R. Corey, RNAi factors are present and active in human cell nuclei, Cell Rep. 6 (1) (2014) 211–221.

[58] Y.L. Chiu, A. Ali, C. Chu, Ying, H. Cao, T.M. Rana, Visualizing a Correlation between siRNA localization, Cellular uptake, and RNAi in living cells, Chem Biol. 11 (8) (2004) 1165–1175.

[59] L.D. Cervia, F. Yuan, Current Progress in Electrotransfection as a nonviral method for gene delivery, Mol. Pharm. Vol. 15 (2018).

[60] F. André, L.M. Mir, DNA electrotransfer: its principles and an updated review of its therapeutic applications, Gene Ther. Vol. 11 (2004).

[61] C. Faurie, M. Rebersek, M. Golzio, M. Kanduser, J.M. Escoffre, M. Pavlin, et al., Electro-mediated gene transfer and expression are controlled by the life-time of DNA/membrane complex formation, J. Gene Med. 12 (1) (2010).

[62] S.A.A. Kooijmans, S. Stremersch, K. Braeckmans, S.C. de Smedt, A. Hendrix, M.J. A. Wood, et al., Electroporation-induced siRNA precipitation obscures the efficiency of siRNA loading into extracellular vesicles, J. Control. Release 172 (1) (2013) 229–238.

[63] R. Stapulionis, Electric pulse-induced precipitation of biological macromolecules in electroporation, Bioelectrochem. Bioenerg. 48 (1) (1999) 249–254.

[64] C.C. Chang, M. Mao, Y. Liu, M. Wu, T. Vo-Dinh, F. Yuan, Improvement in Electrotransfection of cells using Carbon-based electrodes, Cell Mol Bioeng. 9 (4) (2016) 538–545.

[65] J. Duguid, V.A. Bloomfield, J. Benevides, G.J. Thomas, Raman spectroscopy of DNA-metal complexes. I. Interactions and conformational effects of the divalent cations: mg, ca, sr, Ba, mn co, ni, cu, pd, and cd, Biophys. J. 65 (5) (1993) 1916–1928.

[66] S. Haberl, D. Miklavčič, M. Pavlin, Effect of mg ions on efficiency of gene electrotransfer and on cell electropermeabilization, Bioelectrochemistry 79 (2) (2010) 265–271.